Assessment of seagrass percent cover and aboveground carbon stock using linear and random forest regression based on Worldview-2 satellite imagery in Manado City waters, North Sulawesi Province, Indonesia

[1]Maxi W. Solang, [2]Rene C. Kepel, [2]Kakaskasen A. Roeroe, [3]Pramaditya Wicaksono, [2]Winda M. Mingkid, [2]Franky E. Kaparang, [2]Desy M. H. Mantiri, [2]Kurniati Kemer, [4]Muhammad Hafizt, [3]Huwaida N. Salsabila

[1] Marine Science Doctoral Study Program, Faculty of Fisheries and Marine Sciences Sam Ratulangi University, Manado, North Sulawesi, Indonesia; [2] Faculty of Fisheries and Marine Sciences Sam Ratulangi University, Manado, North Sulawesi, Indonesia; [3] Faculty of Geography, Gadjah Mada University, Yogyakarta, Indonesia; [4] Research Center for Oceanography-Research and Innovation Agency, Indonesia (RCO-BRIN). Corresponding author: M. W. Solang, willemsolang@gmail.com

Abstract. The seagrass ecosystem is renowned for making substantial contributions to preserving the balance of marine ecosystems, it offers significant ecological and financial benefits. The rising carbon emissions from several human activities may increase global warming. One method for reducing carbon emissions is to use blue carbon or coastal flora such as seagrass. The seagrass ecosystem has the potential to significantly absorb and store carbon permanently. This study aimed to quantify the density of seagrass Percent Cover (PCv) and aboveground carbon stocks (AGC) in the waters surrounding Manado City, North Sulawesi Province. The survey technique and location were selected with the help of purposeful sampling, while the seagrass data were collected using the line transect quadrant method with an area of 100 x 100 cm^2 to the LIPI seagrass monitoring method. A total of 6 sites was determined for 193 sample plots, consisting of 72 for accuracy calculations and 121 for the regression model. The seagrass carbon stocks were determined using information on the cover percentage. The results showed that 6 types of seagrass were identified, namely *Enhalus acoroides*, *Thalassia hemprichii*, *Syiringodium esoetifolium*, *Cymodecea rotundata*, *Cymodecea serrulata*, *Halodule pinifolia*, and *Halophila ovalis*. *T. hemprichii* and *E. acoroides* accounted for 20.33% of the total cover, each. Station 4 had the highest concentration of seagrass AGC stock, measured by a field sample, at 11.180 g C m^{-2}, while Station 1 had the lowest concentration, measured by a field sample at 6.748 g C m^{-2}. The water area in Manado City fell into the medium category with an average percentage seagrass cover of 50.40%. The seagrass AGC, or total ecosystem carbon store, determined based on the linear regression model, was of approximately 10.773 tons of carbon. In PCv and AGC accuracy analysis, seagrass PCv in B5 had an R^2 value of 0.32, with a linear regression RMSE=25.61%, a Pearson correlation r=0.59, and a Squared Pearson correlation R^2=0.35. The linear regression mapping results showed that PCv was mostly found in the dense class (50–75%) and close to coastal waters. This study suggested that linear regression was a better method than RFR for the seagrass AGC analysis.

Key Words: remote sensing, mapping, aboveground carbon stock, random forest regression.

Introduction. Seagrass, classified as angiosperm, is known to flourish in shallow marine and estuarine environments, thriving while submerged in water. These plants consist of leaves, sheaths, rhizomes (creeping stems), and roots. The research carried out by Wagey et al (2023) identified a total of 8 seagrass species within three coastal waters located in the Minahasa Peninsula, which is situated in North Sulawesi, Indonesia. A study carried out by Supriyadi et al (2023) discovered 8 seagrass species that were documented in Kendari, located in Southeast Sulawesi, Indonesia. Sondak & Kaligis (2022) conducted a research in North Sulawesi, Indonesia, specifically focusing on the

Wori Sub-district, where a total of 6 seagrass species were identified. Seagrass is essential for the ecosystem: as a primary producer, it generates oxygen and organic matter through photosynthesis. Consequently, seagrass beds serve as crucial feeding, spawning, and nursery grounds for marine life (Bortone 2000).

Nienhuis (2002) underscored the significance of the coastal zone in supporting a substantial portion of the living marine resources worldwide, with seagrass being one of the most valuable. Hogarth (2007) further outlined the ecological importance of seagrass environments, delineating the multifaceted roles, including providing breeding and nursery sites for fish, stabilizing sediment, and sequestering carbon. Despite the indispensable ecological functions, seagrass habitats face mounting pressures from both anthropogenic activities and natural impacts (Nadiarti et al 2012). A study reported a loss reaching 30% of seagrass beds in Indonesia (UNEP/GEF 2004). The significance of seagrass is underscored by the Seagrass Condition Assessment Monitoring Guidebook (Rahmawati et al 2017). The diverse roles include acting as a filtering medium for shallow seawater, providing habitat for various marine biota namely baronang/ingkis fish, shellfish, crabs, and sea cucumbers. Seagrass serves as a breeding ground for juvenile marine life, offers sustenance for humans, provides refuge for endangered species including dugongs and turtles, while also mitigating beach erosion by reducing wave energy. Moreover, these plants contribute to climate change mitigation and adaptation. Seagrass meadows, as elucidated by Mckenzie & Yoshida (2009), are exceptionally productive ecosystems, offering up to 27 times more habitable substrate than non-vegetated areas. Previous studies show that seagrass meadows host approximately 40 times more creatures than dry sand areas (Humphries 1991; Acosta 1999; Bologna & Heck 2002; Kendrick 2002; Merryanto et al 2022). Understanding the spatial distribution and characteristics of seagrass resources is crucial for an effective management. Coastal managers require detailed maps depicting the occurrence and abundance of species, as insights into the details of the response to human-induced changes, and information on the potential for the restoration of damaged meadows (Savini & Gai 2023; Uku et al 2021). Informed management decisions about recovery, restoration, and the facilitation of natural spatial dynamics necessitate knowledge of historical seagrass distribution (McKenzie 2003). Coastal managers must consider where seagrass may have existed historically to devise comprehensive strategies for sustainable management. This knowledge will contribute to the conservation and sustainable use of the ecosystem.

To effectively map the aboveground carbon (AGC) stock of seagrass by integrating remote sensing and field data, comparable field data are crucial. These field data serve the dual purpose of training the regression model and assessing the accuracy of the resultant map (Hossain et al 2015; Tamondong et al 2018). However, acquiring such data through conventional means is problematic due to its damaging, expensive, and time-consuming nature. This underscores the pressing need to devise a rapid, non-destructive approach for estimating AGC in seagrass, which can be used in training and validating remote sensing-based AGC mapping techniques (Misbari 2017). To address the escalating environmental degradation, it has become increasingly important to accurately map both the distribution and quantity of seagrass. These mapping endeavors hold significant value for coastal area management and conservation strategies. Remote sensing technology, renowned for its accessibility and wide coverage, has been a staple for decades in mapping and monitoring coastal and shallow marine environments. By leveraging image processing techniques and insights into potential carbon reserves within seagrass beds, remote sensing facilitates the management of carbon stores in coastal regions and small islands (Rais et al 2023; Green et al 2000). Successful applications have enabled the mapping of key metrics such as leaf area index, seagrass PCv, and AGC stock (Wicaksono & Hafizt 2013; Wicaksono et al 2019a; Wicaksono et al 2021). These advancements have paved the way for a comprehensive understanding of seagrass ecosystems and the carbon storage potential.

This study aimed to estimate AGC seagrass information utilizing easily measurable PCv data and to create maps at community levels using WorldView-2 images. To achieve this, two specific objectives were proposed: (1) estimating AGC seagrass from the PCv at the community level, and (2) evaluating the accuracy of the resulting maps. This

investigation focused on the waters adjacent to Manado City in North Sulawesi Province, aiming to quantify the density of seagrass cover percent (PC) and AGC stocks in seagrass.

Material and Method

Description of the study sites. This research was carried out in the waterways of Bunaken District, Manado City, within the North Sulawesi Province (Figure 1). Seagrass species such as *Thalassia hemprichii* and *Enhalus acoroides* thrive in shallow waters with sandy and muddy bottoms. Additionally, other species including *Syiringodium isoetifolium*, *Cymodecea rotundata*, *Cymodecea serrulata*, *Halodule pinifolia*, and *Halophila ovalis* inhabit the area.

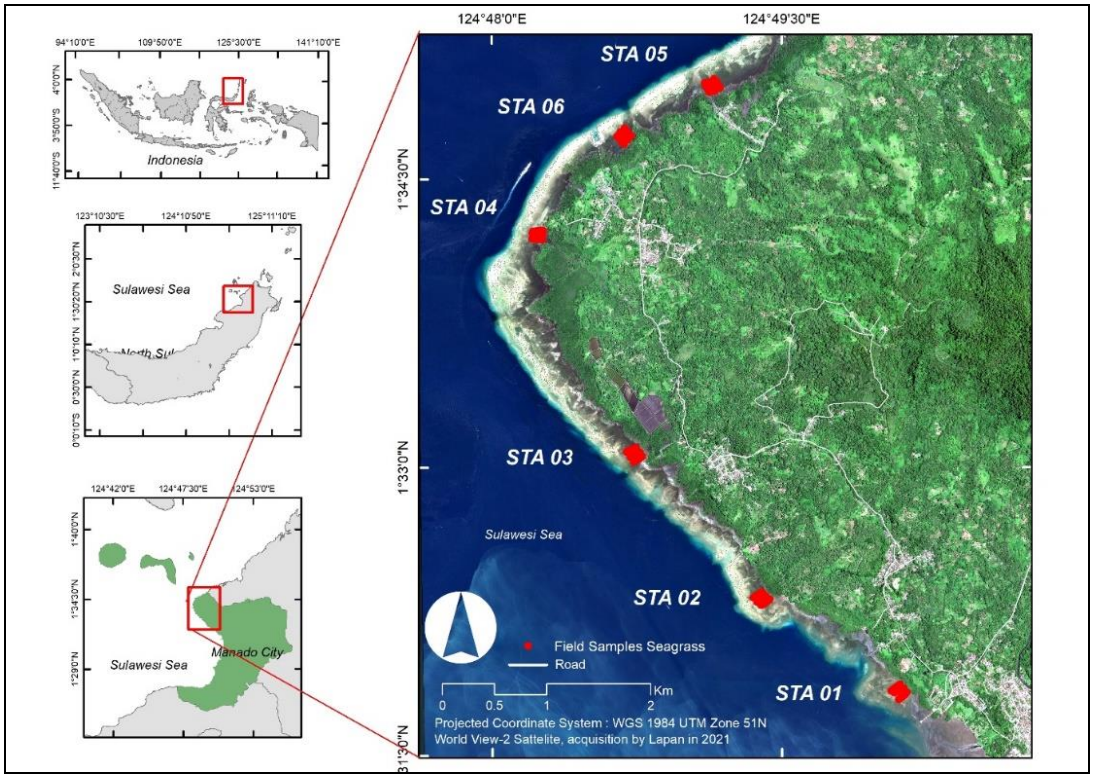

Figure 1. Map of the study area.

Seagrass beds have various configurations depending on the species present, appearing either as continuous, mixed, or patchy formations. Benthic organisms, including coral reefs and macrobenthos, coexist in the study area. The seagrass ecosystems under investigation were located specifically within the Bunaken National Park (TN) area, as designated by the Minister of Forestry's Decree Number: SK. 734/Menhut-II/2014 (Government of Indonesia 2014). According to the Regional Regulation of North Sulawesi Province Number 1 of 2017 (North Sulawesi Province 2017), known as the Zoning Plan for Coastal Areas and Small Islands of North Sulawesi Province (RZWP3K), spanning over the period 2017-2037, these seagrass ecosystems fall within the Conservation Area. Based on Regional Regulation Number 1 of 2023 (Manado Municipal Government 2023), which pertains to the Regional Spatial Plan of Manado City (RTRW) for the years 2023-2042, these ecosystems are situated within the Protected Area of the Bunaken National Park management region. The area has diverse geomorphic benthic habitats, including reef flat, back reef, reef crest, fore reef, and cliff formations. Seagrass beds predominantly occur on the coastline, intermixed with substrates classified into four types, namely muddy, sandy, rubble, and reef flat. This complex substrate composition posed a challenge for accurate mapping efforts.

Field data collection and handling. A total of 6 study stations (ST) were established within the waters of Manado City, from which a total of 193 samples measuring seagrass cover percentages were collected. These samples were divided into 121 data points for constructing the regression model and 72 for accuracy assessment (Figure 2). Field data on percent seagrass cover were obtained using the photo-square technique, with 1 m² plot sizes within seagrass beds, along with photo-transect techniques (Roelfsema et al 2014). The seagrass cover percentage refers to the projected horizontal coverage in square units, estimated based on the identified species within the sampled areas. The locations for sampling were determined by observing variations in cover apparent in the original composite remote sensing imagery (true color RGB 5,3,2). The identified seagrass species within the study area included *E. acoroides*, *T. hemprichii*, *Syiringodium esoetifolium*, *C. rotundata*, *C. serrulata*, *H. pinifolia*, and *H. ovalis*. These samples were crucial in estimating the AGC derived from seagrass PCv at the community level.

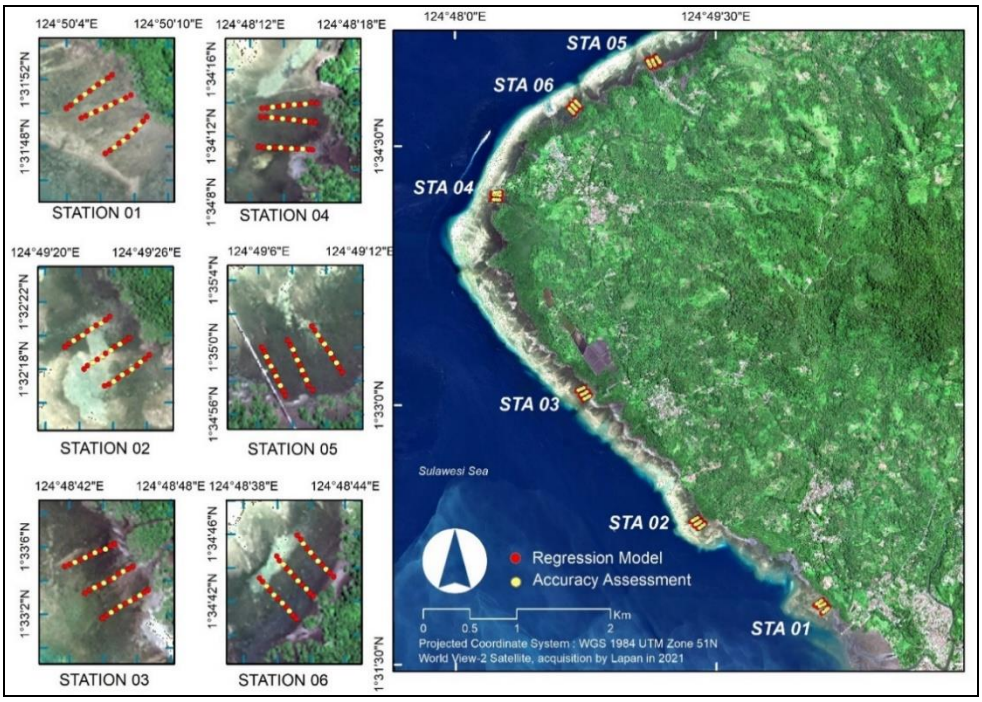

Figure 2. Location map of regression models and accuracy test samples.

This study used simple linear regression analysis to determine the linearity of the dependent variable with the independent. The relationship between the seagrass cover and the raster value of WorldView-2 imagery in each band produced the best equation for modeling the PCv map. Similarly, the amount of AGC was regressed with the raster value of WorldView-2 imagery in each band. The best regression results were applied to the seagrass AGC mapping model. The next step was to classify the percentage of seagrass cover created with the random forest regression (RFR) algorithm, using the EnMAP-Box 2.2.1 plugin. The input used was the result of seagrass masking through the WV-2 image. Furthermore, the regression and test samples were used as inputs in making the carbon stock estimation map. AGC maps were obtained using the RFR algorithm, which utilized a set of decision tree classifiers to classify data. Integrated in-situ benthic habitat data and processing of WorldView-2 (WV2) image were used to parameterize the machine-learning algorithm (RF). Based on previous reports, it is recommended to use the more general classification scheme to avoid several issues regarding benthic habitat variations. The result also established the possibility of mapping a benthic habitat without the use of training areas. Moreover, image processing was conducted using an RFR algorithm in mapping seagrass carbon stocks.

A collection of decision tree classifiers was used by the RF algorithm to categorize data. To parameterize the machine-learning algorithm (RF), Wicaksono et al (2019b) combined the image processing of WorldView-2 (WV2) images with the in situ data on

the benthic habitat. To avoid several problems related to changes in the benthic habitat, a more general classification scheme should be used in the RF model. The outcome also demonstrated that a benthic environment might be mapped without the need for training areas. Rais et al (2023) also studied the mapping of seagrass carbon stocks by image processing with an RFR approach.

Image correction. Atmospheric correction was carried out to reduce errors caused by disturbances such as scattering due to gases contained in the atmosphere. This stage used the Fast line-of-sight Atmospheric Analysis of Spectral Hypercubes (FLAASH) method implemented through the image processing software (ENVI 2009). The model input parameters included the initial visibility=77km, the atmospheric model: tropical, off-nadir angle's average=18.68834, with an image location in the Manado City area. FLAASH is an absolute atmospheric correction method that considers in more detail conditions such as aerosols at the time of recording. The raw data image used as input was calibrated in radian values, resulting in the unit of μW $cm^{-2}sr^{-1}nm^{-1}$ while the corrected WorldView-2 image is shown in Figure 3.

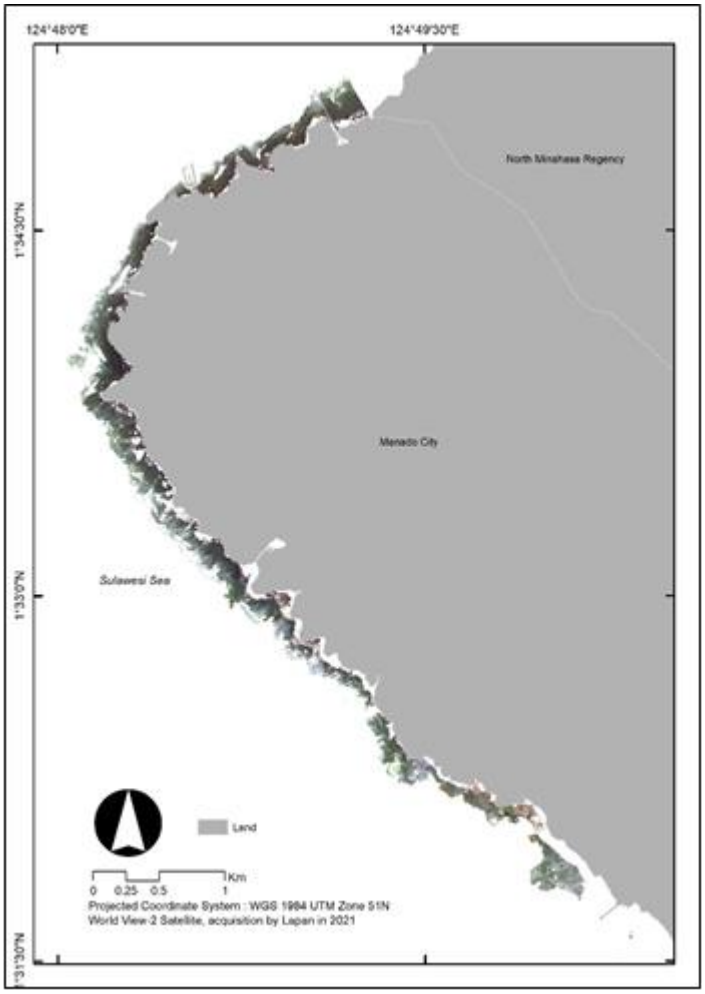

Figure 3. Masking satellite imagery of the study area and spatial distribution of seagrasses with natural/true color (band 532).

The minimum negative value in each image channel could be considered a recording error because the number of pixels with a negative value was lower in the image scene. The results of the FLAASH correction map were then converted to a digital number range of 0-1 and applied to all bands with the equation:

(b1 le 0)*0+(b1 ge 10000)*1+(b1 gt 0 and b1 lt 10000)*float(b1)/10000

The WorldView-2 Multispectral Imagery (1.8 m, 8 bands, Level 2A) comprises 4 standard bands of red, green, blue, and near-infrared1, plus 4 bands of coastal, yellow, red edge, and near-infrared2. The sun glint correction process in the bands was observed and significantly altered the reflections of the benthic habitat in most parts of the scene, to a minimum. Removal was carried out using a formula incorporating the near infrared band as described in Hedley et al (2005) and Kay et al (2009). The WorldView-2 image specification has 2 near-infrared bands, selecting the best near-infrared band to correct sun glint in the visible band. Each visible band was regressed in both near-infrared bands. The data for the regression analysis comprised the optical reflection of deep water at various sunlight intensities. Furthermore, the regression analysis was carried out to obtain the slope of the regression (calibration gradient) required to eliminate sunlight in the visible band using the near-infrared band (Wicaksono 2016; Wicaksono & Hafizt 2013). Water column correction was not carried out because the conditions during the satellite image recording were in the low tide range, hence, some locations in the seabed were shallow and the seagrass ecosystem was exposed to the surface. Ampou et al (2018) showed that for the benthic habitat in Bunaken Island it is not necessary to carry out a water column correction, due to the narrow range of depths found in the reef flat. Another study conducted by Ilyas et al (2020) reported that the application of treatments with and without water column correction in mapping benthic and seagrass habitat ecosystems using several classification algorithms produced accurate, but not significantly different results. The topographic conditions of the study area correspond to the 2nd-order polynomial transformation. In the rectification stage, the resample type was cubic convolution and the number of GCPs required for geometric correction was eight points. The geometric correction was conducted through the image-to-image method to associate the pixels on the satellite image with the actual location on Earth with a total RMS error of 0.689207. Furthermore, the image orthorectification process used the WorldView-2 image map acquired in 2015, with a spatial resolution of 0.5m for the Manado City Detailed Spatial Plan (RDTR) which has been orthorectified by the Geospatial Information Agency with a scale of 1:5000. Ground control points (GCPs), identifiable features such as docks, road intersections, building corners, and others were used for a more precise mapping. Map accuracy was based on Geospatial Information Agency Regulation Number 6 of 2018 concerning Amendments to Regulation Number 15 of 2014 concerning Technical Guidelines for Base Map Accuracy (HGIA 2018). The orthorectification results with a Total RMS Error of 0.689207 was achieved on a scale of 1:2500, meeting the criteria for a class one map accuracy.

A summary of the WorldView-2 image's characteristics used in this study is presented in Table 1.

Table 1

WorldView-2 image specifications

Characteristics	*Information*
Image name	WorldView-2
Acquisition time	May 25, 2021
Spatial resolution	<pixelHeight>2.077 m <pixelWidth>1.988 m
Spectral resolution	Band Coastal blue (B1), Wavelength: 400 to 450 nm Band Blue (B2), Wavelength: 450 to 510 nm Band Green (B3), Wavelength: 510 to 580 nm Band Yellow (B4), Wavelength: 585 to 625 nm Band Red (B5), Wavelength: 630 to 690 nm Band Red Edge (B6), Wavelength: 705 to 745 nm Band NIR-1 (B7), Wavelength: 770 to 895 nm Band NIR-2 (B8), Wavelength: 860 to 1040 nm Panchromatic, Wavelength: 450 to 800 nm
Radiometric resolution	16-bit
System coordinates	UTM Zone 51N

The WorldView-2 image used in this study was acquired by the National Aeronautics and Space Administration (NASA) on May 25, 2021, and subsequently provided to the government. This acquisition occurred at 14:44 GMT local time, capturing the Manado City area with the sun azimuth at 44.638493 and an elevation of 61.96089. The image comprised conventional water penetration bands blue, green, and red alongside three novel bands cyan, yellow, and red. The inclusion of these bands was crucial for extracting information from the intricate seagrass ecosystems due to the ability to penetrate different depths based on light and water conditions. The image acquisition process used 2 bytes per pixel, with a 16-bit radiometric resolution and 2-meter spatial resolution. However, it is important to acknowledge the 11-bit (0-2048) natural dynamic range of WorldView-2 images. Despite the recent availability of WorldView-3 imagery, offering additional features, the quantity of water penetration bands is comparable to that of WorldView-2 (DigitalGlobe 2016). The distinguishing factor lies in its introduction of shortwave infrared band sets.

Benthic habitat mapping*.* The seagrass mask was created from a visual interpretation based on local knowledge and direct field observation. Processed satellite images were then categorized using an unsupervised Isodata algorithm approach of 17 classes with Envi software. Afterwards, the results of the Isodata algorithm approach for unsupervised classification were eliminated, leaving only the area identified as seagrass class. Furthermore, the results of ground truth samples were used to compare with the resulted seagrass classes, and the geoprocessing was carried out with the ArcMap software. Multiple input datasets were combined into a single, new output dataset. This tool can combine point, line, polygon feature classes, or tables. The calculation results estimated the seagrass area in Manado City waters to be ±136.75 ha.

Seagrass PCv mapping. The method used in the seagrass monitoring activities at the study site was a quadratic transect, perpendicular to the shoreline (McKenzie et al 2003; McKenzie 2003), and consisting of transects as well as frames. The transect is a straight meter line drawn over the seagrass bed, while the square is an equilateral rectangular frame placed on the line. Seagrass cover was interpreted directly in the field, and the results of the plots were geotagged with the Zone 51 N UTM coordinate system from the Garmin Oregon GPS Type 750. Assessment and identification of seagrass cover was conducted using standards (Rahmawati et al 2017). Assessors observed the characteristics of the substrate visually and by twisting using the hands, then observed that the characteristics of the substrate were divided into muddy, sandy, rubble (coral fragments), and reef flat.

Seagrass AGC mapping*.* Seagrass species with a higher percentage value of closure were more dominant on the permanent monitoring transect at the observed station. The next step was to estimate the AGC of the seagrass. Calculation of seagrass carbon stock was carried out using an allometric approach based on the regression equation (Wicaksono et al 2021) presented in Table 2. The calculation was performed by measuring the actual cover of seagrass species in the field to obtain data, which were then converted into a regression equation. Seagrass species are mapped to perform the masking on the AGC mapping.

Table 2

Seagrass aboveground carbon stocks (AGC) equation

No	*Species of seagrass*	*Formula*	*References*
1.	*Enhalus acoroides*	$y=0.3179(PC_{Ea})+0.6295$	Wicaksono et al (2021)
2.	*Thalasia hemprichii*	$y=0.1069(PC_{Th})+0.0951$	
3.	*Syiringodium esoetifolium*	$y=0.00268(PC_{Se})-0.0022$	
4.	*Cymodecea rotundata*	$y=0.0604(PC_{Cr})-0.1767$	
5.	*Halodule pinifolia*	$y=0.0604(PC_{Hp})-0.1767$	
6.	*Halophila ovalis*	$y=0.00268(PC_{Ho})-0.0022$	

Linear regression. In simple linear regression, a criterion variable was predicted from one predictor (Baeza-Serrato & Vázquez-López 2014). Wicaksono & Hafizt (2013) conducted a regression analysis between seagrass PCv and leaf area index (LAI) at the community and species levels. The study used simple linear regression to compare the PCv values of seagrasses in the field with the raster values on WV-2 satellite imagery. A similar procedure was performed for seagrass AGC in the field and rasterized values on WV-2 satellite imagery. The best equation results were used to model the PCv and AGC maps. The analysis was then continued to compare the modeling of PCv and AGC maps using Machine-Learning RF.

Random forest regression (RFR). The RF algorithm used in this study was based on Breiman (2001). RF is an ensemble classification method for classifying trees and the algorithm can produce a good classification result even though there are many outliers in the training (Pal 1996). To obtain the RFR model, the RF algorithm was tuned using the following parameters: (1) dataset regression, validation sample, and image satellite, (2) a number of trees=100, (3) a number of feature parameters and the square root of all features. The Fast Accuracy Assessment of an RFR model will show three windows. The first produces a textual report of the residual statistics, including the values for RMSE, Pearson correlation r, and Squared Pearson correlation R^2.

Accuracy assessment. The accuracy test in this study used Root Mean Squared Error (RMSE), Pearson correlation (r), and Squared Person correlation (R^2) performed on the PCv map and AGC map.

Flowchart. A study flowchart can help understand and illustrate the key steps required in this process. In this context, the flowchart (Figure 4) offers guidance on the measurement and analysis steps required to evaluate the seagrass cover percentage and estimate the amount of stock carbon stored aboveground using satellite imagery.

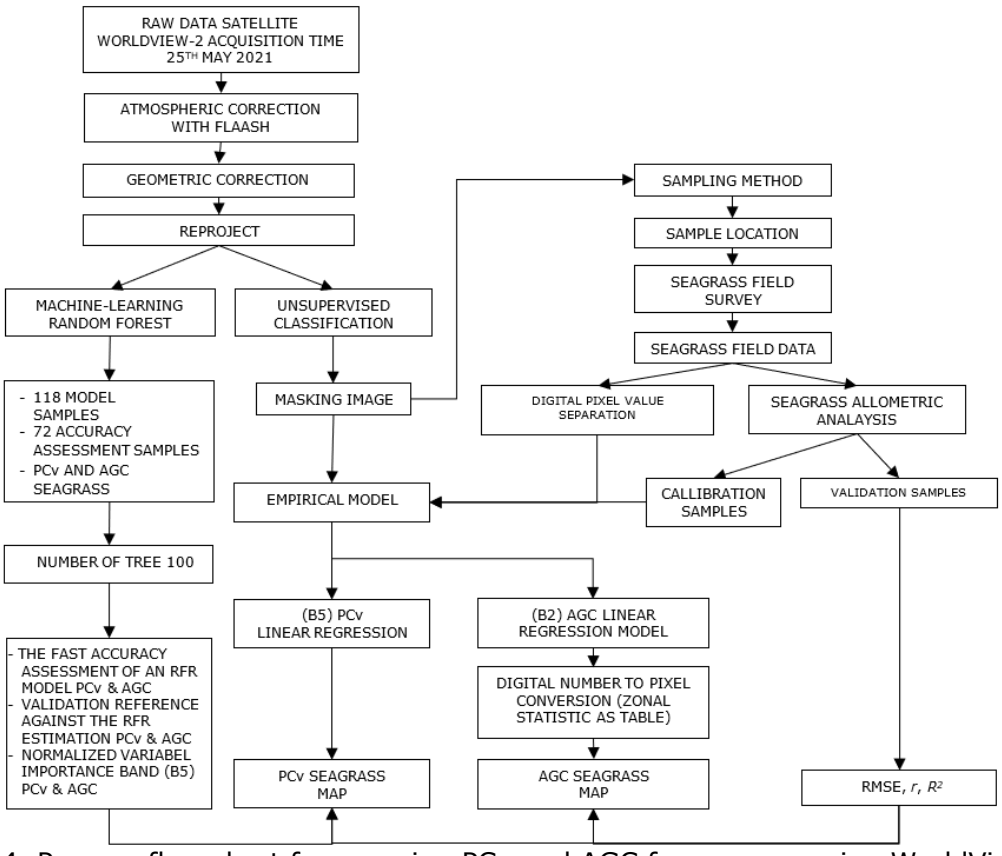

Figure 4. Process flow chart for mapping PCv and AGC fo seagrass using WorldView-2's passive remote sensing technology.

Results. According to the Seagrass Assessment Monitoring Guide, Edition 2, developed by the Oceanographic Research Center-LIPI (Rahmawati et al 2017), the Manado City water area has an average seagrass cover of 50.40%, placing it within the medium category. Figure 5 shows the percentage distribution of seagrass cover and the prevailing species' type. Station 4 recorded the highest value at 76.49%, predominantly characterized by *T. hempricii* at 20.14%. Conversely, Station 1 had the lowest coverage at 30.94%, with the dominant species being *H. ovalis* at 0.21%. As shown in Figure 5, significant differences in seagrass coverage were observed across various sites. Specifically, ST4 had the most extensive onsite coverage at 76.49%, while ST1 showed the least coverage at 30.94%.

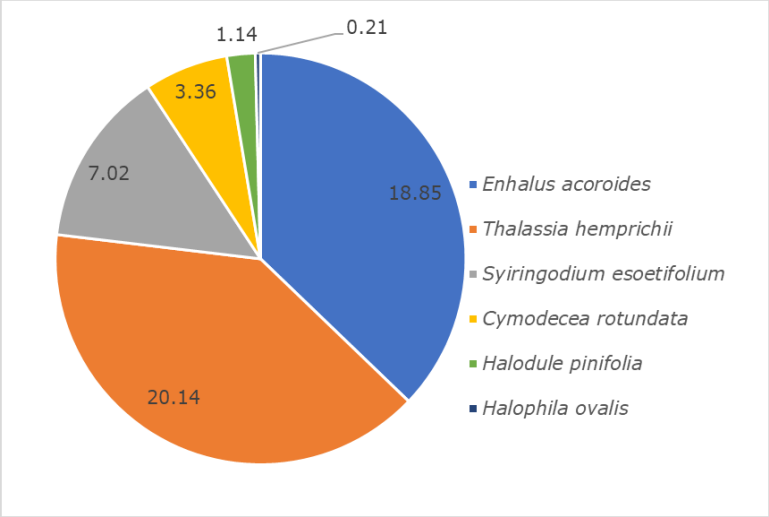

Figure 5. Dominance of seagrass species.

Photos of several types of seagrass species found in the waters of Manado City are presented in Figure 6.

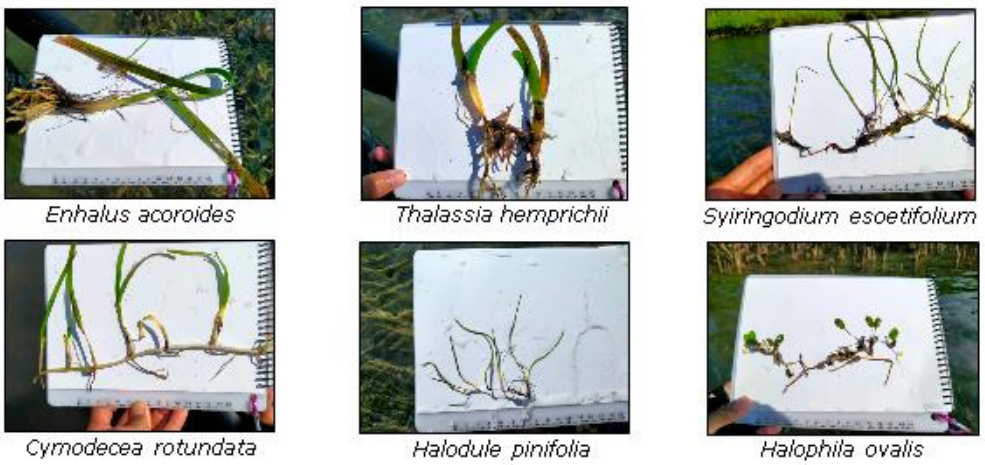

Figure 6. Photos of seagrass species.

Environmental parameters result. Seagrass ecosystems in the waters of Manado City play a critical role in coastal habitats and are influenced by a myriad of interacting environmental and physical factors. Environmental parameters include the surrounding conditions, while physical parameters comprise water temperature, salinity, and pH levels. Optimal water temperature is crucial for seagrass growth and reproduction, but extreme fluctuations can induce stress and even result in death. Similarly, water salinity plays an essential role, as seagrasses thrive within specific ranges. Some areas within the plots showed slight turbidity due to sediment mixing with the substrate. Table 3 and

Figure 7 present the sampling of PCv, AGC, as well as environmental and physical parameters affecting seagrass ecosystems. PCv data was obtained from the result of assessing the percentage of seagrass density in each transect/plot and then averaged. Meanwhile, AGC estimation was analyzed using the equation (Wicaksono et al 2021) and PCv. The analysis results of both were then modeled with the raster value of the WV-2 image using the linear regression method. The observed physical parameters across all stations had a consistent range with temperatures falling within 31.3 to 34.6°C, salinity of 30 ppm and 34 ppm, while the pH values varied between 7.46 and 8.

Table 3

Environmental parameters

Station	*Time*	*Weather*	*Mangrove*	*Brightness*	*Dock*	*River*	*Residents*	*Depth*	*Activity*
ST1	10.30-12.30	Sunny	A	Simply	NA	NA	NA	0-20 cm	None
ST2	9.30-11.45	Sunny	A	Simply	NA	NA	NA	5-15 cm	None
ST3	9.50-11.50	Sunny	A	Simply	NA	NA	NA	0-20 cm	None
ST4	9.50-11.50	Sunny	A	Simply	NA	NA	NA	0-25 cm	None
ST5	12.05-14.10	Rainy	A	Slightly turbid	A	NA	A	5-30 cm	A
ST6	12.15-14.05	Sunny	A	Simply	A	NA	NA	10-50 cm	None

A-available; NA-not available.

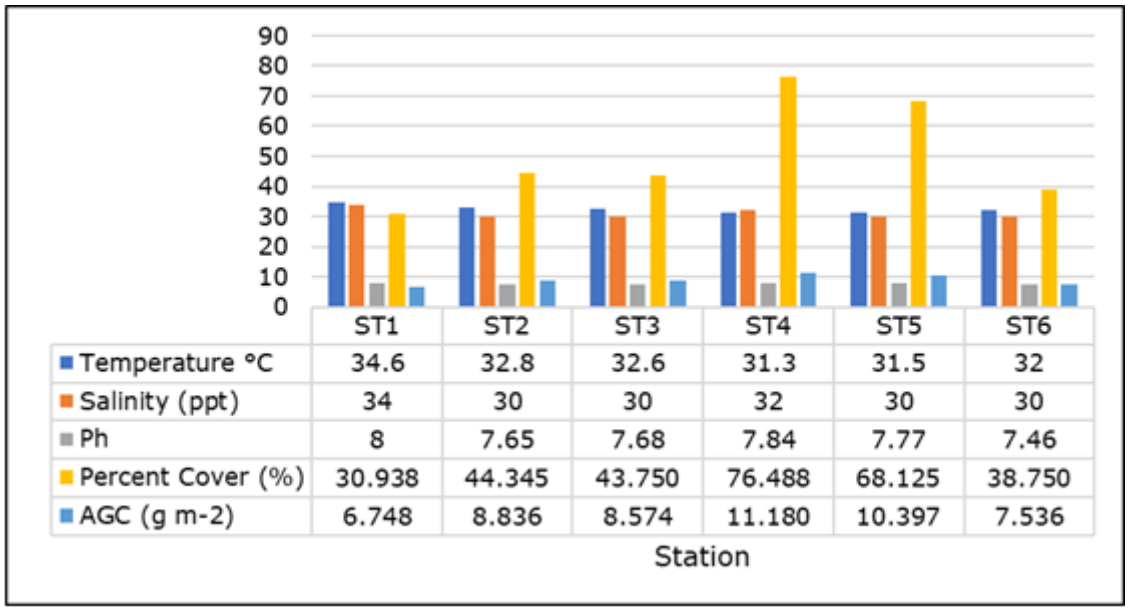

Figure 7. Physical parameters PCv and AGC of seagrass.

Photo quadrant result. Data collection was carried out on three transects with a length of 100 m each and an interval of 50 m (Figure 8), resulting in a total area of 100 x 100 m^2. Quadratic frames were placed on the right side of the transect at a distance of 10 m from each other, totaling 11 squares on each transect. The starting point was placed at a distance of 5–10 m from the first point where seagrass was encountered, starting from the coast.

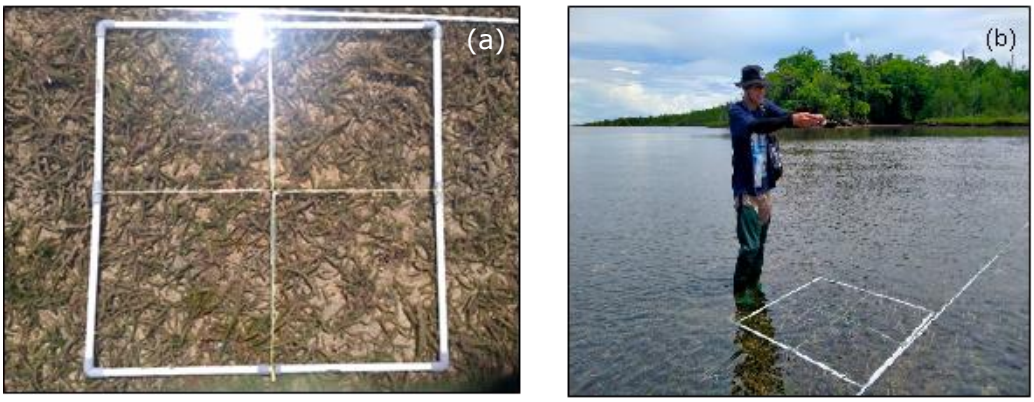

Figure 8. (a) Photo of plot quadrant size 1 m^2, (b). Photo of seagrass sampling process.

Seagrass Percent Cover linear regression. The regression analysis conducted using satellite image raster values B1-B8 (Table 4), in comparison to the PCv of seagrass observed in the field, showed that B5 had the highest R^2 value of 0.328 (Figure 9). The specifications of the Red 5 Band (630-690 nm) (DigitalGlobe 2009) primarily focused on the absorption of red light by chlorophyll in healthy plant material. PC of seagrass in the field showed that B5 had the best R^2 of 0.328. The equation results of B5 y=(-905.51*B5)+82.169 were modeled in the distribution map and then classified in the PCv map of seagrass distribution, based on the Seagrass Cover Category (Rahmawati et al 2017). The empirical modeling of PCv using WorldView-2 image was performed with the linear regression analysis. The spatial distribution was the highest around ST4 and the lowest at ST1. The results of linear regression mapping showed the dominant seagrass PCv in the dense class (50%-75%) and located along the coastal waters (Figure 10).

Table 4

Equation regression PCv

Band	*Equation*	*R^2*
Band 1	y=-2150x+70.252	0.229
Band 2	y=-1538.3x+97.426	0.316
Band 3	y=-838.36x+83.336	0.262
Band 4	y=-749.1x+80.967	0.267
Band 5	y=-905.51x+82.169	0.328
Band 6	y=87.292x+46.703	0.005
Band 7	y=186.92x+41.367	0.044
Band 8	y=220.94x+47.834	0.009

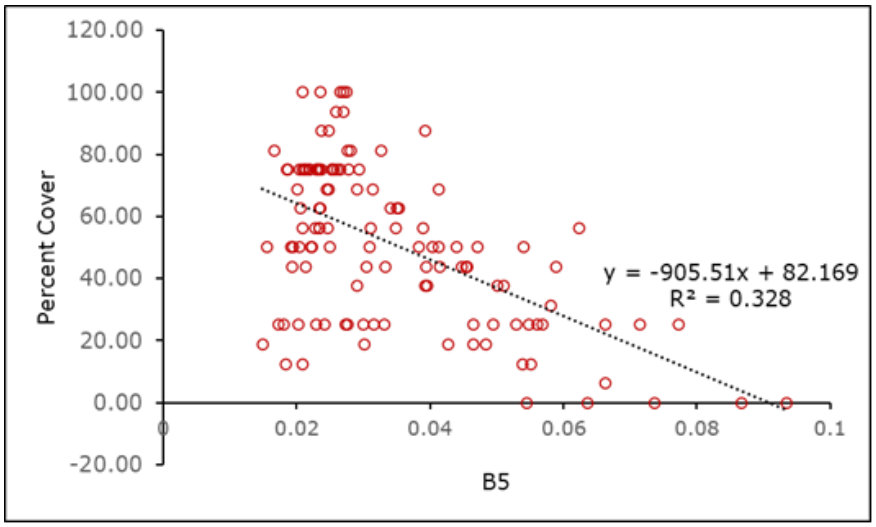

Figure 9. Plot of the B5-based seagrass distribution vs the seagrass PCv.

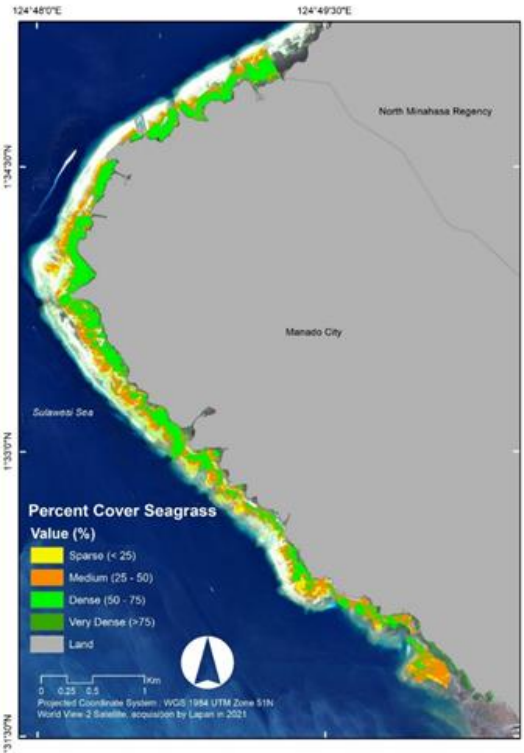

Figure 10. Linear PCv of seagrass map; RMSE=25.61%, Pearson correlation r=0.59, Squared Pearson correlation R^2=0.35.

Random forest. The results of RFR mapping of seagrass PCv estimation using EnMAP-Box 2.2.1 software are shown in Figure 11. RF had a dominant seagrass PCv in the dense class (50%-75%), scattered on the coastal areas. This shows a difference with the results of the linear regression in the dense class.

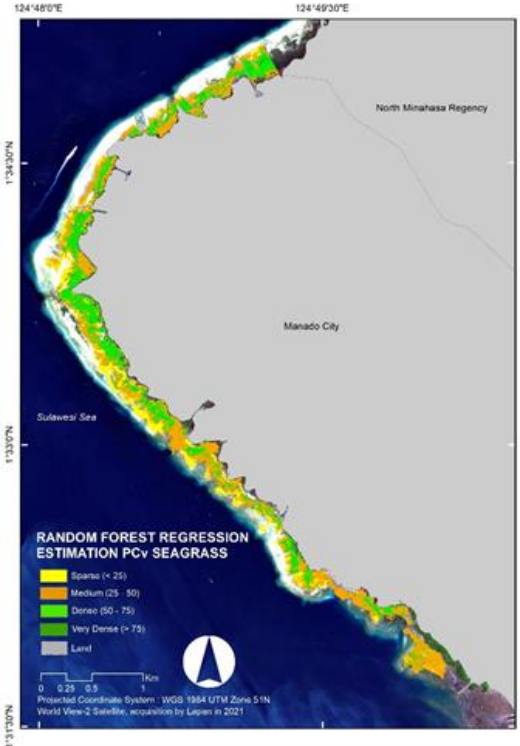

Figure 11. RFR estimation map of Seagrass PCv; RMSE=25.87%, Pearson correlation r=0.63, Squared Pearson correlation R^2=0.40.

The scatter plot showed values of the validation reference against the RFR PCv estimation in Figure 12. Based on the graphical plot of the reference data and the estimation trend, the PCv estimation results have an underestimated value.

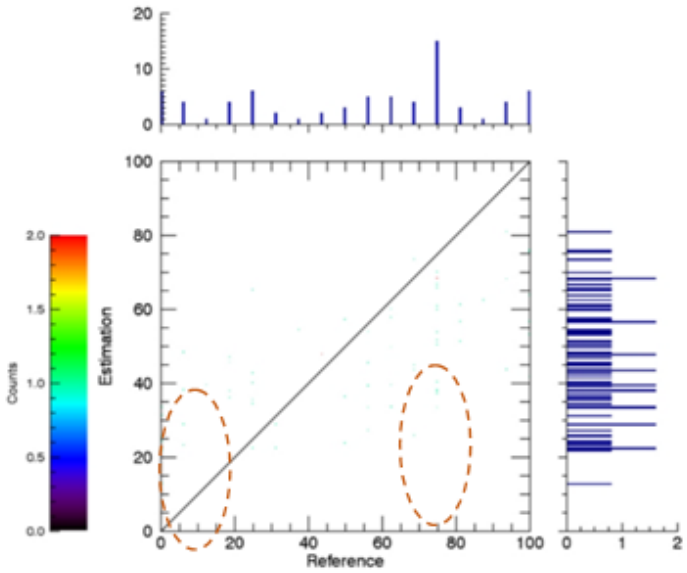

Figure 12. Graph of the validation reference against the RFR PCv estimation.

The estimation model's values do not increase at the same rate as the reference value, due to the blurred image factor, as seagrass and muddy waters were not well separated. Mangrove ecosystems also have an influence due to the mud substrate, affecting the extraction of pixel values to obtain the best R^2 value. Another influential factor was the absence of water column correction in the satellite images. The medium seagrass PCv area near the shoreline further added complexity to the analysis. The values should be positioned along the diagonal, showing that all estimated values were equal to the reference. The graph below shows that Band 5 (B5=red) is most commonly used in RF iterations (Figure 13).

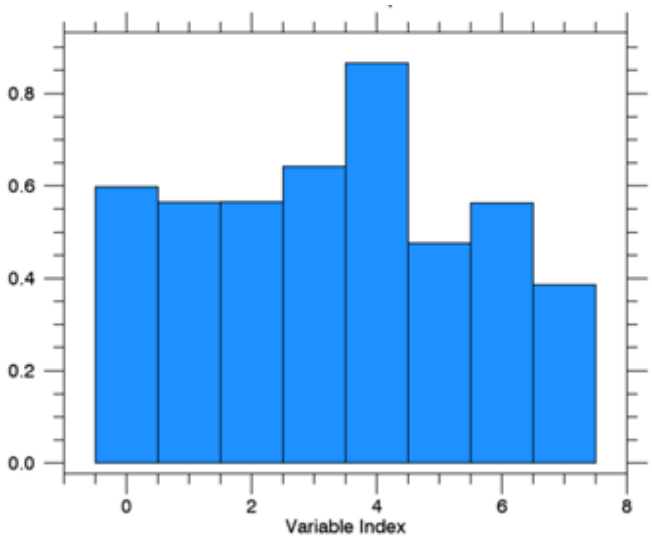

Figure 13. Normalized variable importance in the RFR model of seagrass PCv (the variable index stands for the color band, B1 to B8).

Seagrass reflectance has certain spectral characteristics that reflect light, including the red band. Image analysis in the red band can help identify and map seagrass locations (Rahman & Wicaksono 2019). Previous RMSE analysis showed that

PCv mapping using a linear regression approach provided better results than RFR modelling, although not significantly different.

AGC seagrass linear regression. The process of extracting the raster value of each band from B1-B8 was regressed with the total seagrass AGC to produce a predicted equation for each band. The results for each band were obtained by extracting the raster value of the WV-2 satellite image with each pixel of the test and of the regression model sample. By using a correlation analysis between the raster value (x-axis) of each band, compared to the total AGC g C m^{-2} (y-axis), the best regression result was found for the Band Blue (B2), with the wavelength: 450 to 510 nm and R^2=0.3759. The regression graph of raster values B1-B8 with seagrass AGC is shown in Table 5.

Table 5

Equation regression AGC

Band	*Equation*	*R^2*
Band 1	y=-379.85x+12.368	0.3278
Band 2	y=-247.7x+16.436	0.3759
Band 3	y=-133.49x+14.109	0.3055
Band 4	y=-119.49x+13.741	0.3125
Band 5	y=-142.7x+13.872	0.3741
Band 6	y=-10.639x+9.377	0.0033
Band 7	y=10.513x+8.3792	0.0064
Band 8	y=-4.9395x+8.9619	0.0002

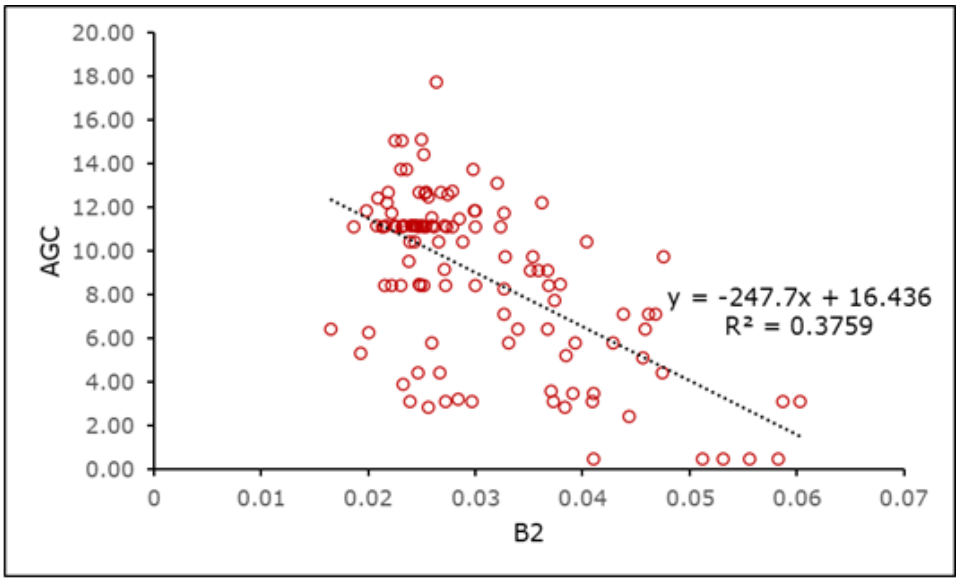

Figure 14. Plot of the B2-based seagrass distribution vs the AGC of seagrass.

The R^2 value of 0.3759, implies that about 37.6% of the variation in the dependent variable can be explained by the independent variable in the regression model used, while the raster value band results were used to calculate the RMSE (Figure 14). The specifications of the Blue band (450-510 nm) (DigitalGlobe 2009) include: 1). Readily absorbed by chlorophyll in plants, 2). Provides good penetration of water, 3). The Blue band is less affected by atmospheric scattering and absorption compared to the Coastal Blue band.

The results of the B2 regression model in Figure 14 were then converted to pixels by eliminating all Digital Number (DN) less than 0. Using a raster calculator, the eliminated map was multiplied by the pixel area WV-2=4.12 m^2 (rounded down to 4 m^2). Further processing was conducted using zonal statistics as a table tool in the ArcMap software to calculate statistics on values of a raster within the zones of another dataset.

The results of the calculations showed a total seagrass AGC of 10.773 ton carbon. The spatial distribution was highest around ST4 and lowest at ST1. The seagrass AGC classification map was divided into five classes, as shown in Figure 15.

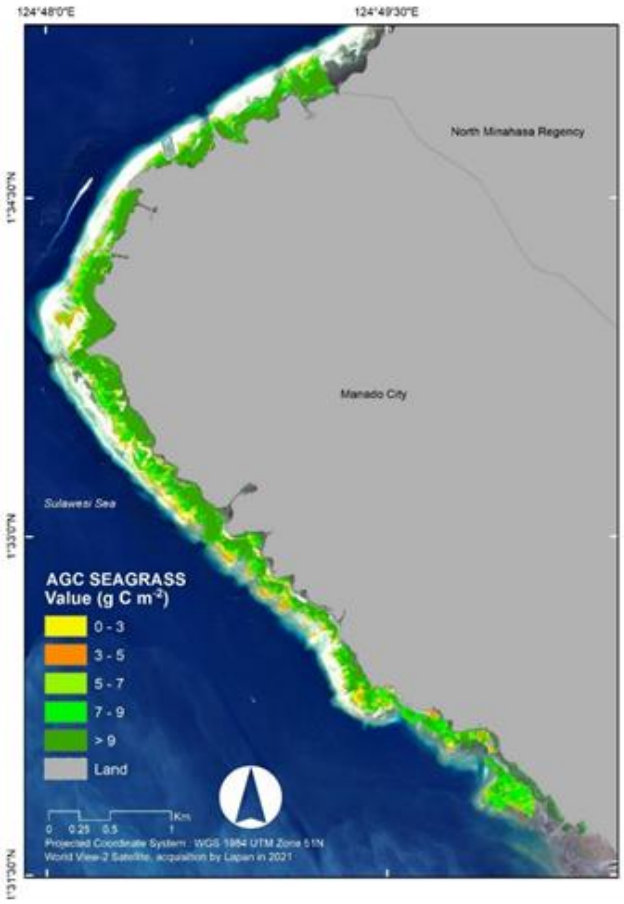

Figure 15. Linear AGC seagrass mapping at the community level, with RMSE=3.708 g C m^{-2}, Pearson correlation r=0.57, Squared Pearson correlation R^2=0.33

The linear regression mapping results had dominant seagrass AGC in the >9 g C m^{-2} class and were scattered along the coastal waters. The next step was to calculate the RMSE, representing the AGC estimation of each prediction accuracy. This was conducted by calculating the AGC model data and field test/validation results.

Random forest. ImageRF is an Interactive Data Language (IDL) based tool for the supervised classification and regression analysis of remote-sensing image data. It implements the machine-learning approach of RF (Breiman 2001) that uses multiple self-learning decision trees to parameterize models for estimating categorical or continuous variables. The results of RF mapping had dominant seagrass AGC in the >9 g C m^{-2} class, and were located scattered along the coastal waters of Manado City (Figure 16). In the linear regression map, dominant seagrass was found in the waters of Tongkaina Village, Bunaken District to the north compared to the RFR map for the same location.

The scatter plot shows values of the validation reference against the RFR estimation. Based on the plot graph of the reference data and the estimated trend in Figure 17, the estimated AGC result had an underestimated value. As the reference value increased, the estimation model did not generate a comparable trend. In an ideal scenario, the value should be positioned along the diagonal, showing that all estimated values are equal to the reference (Wicaksono & Harahap 2023). Given that the muddy seas and seagrass were not clearly separated, the blurred image component caused the reference validation value of the RFR AGC estimation result to be underestimated. This impacted the extraction of pixel values, obtaining a suboptimal R^2. The AGC region of

medium seagrass abundance, close to the coast, further added to the complexity of the analysis.

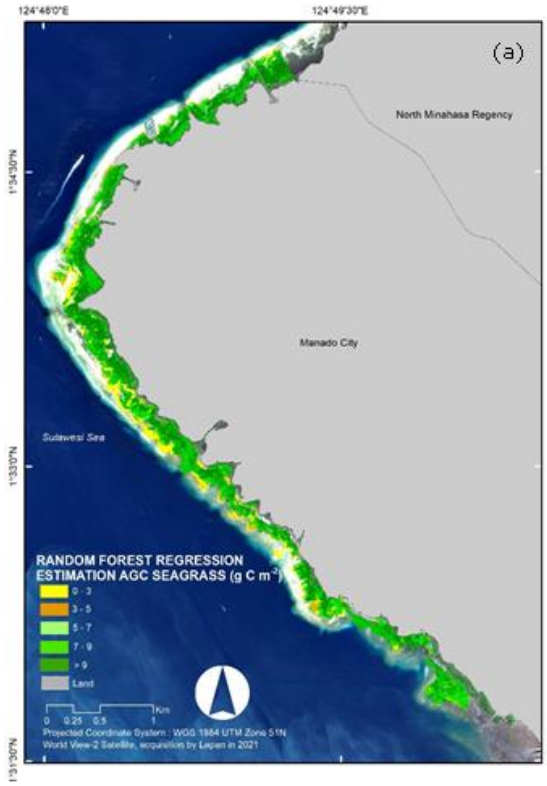

Figure 16. RFR estimation map for the seagrass AGC; RMSE=3.742 g C m^{-2}, Pearson correlation r=0.60, Squared Pearson correlation R^2=0.36

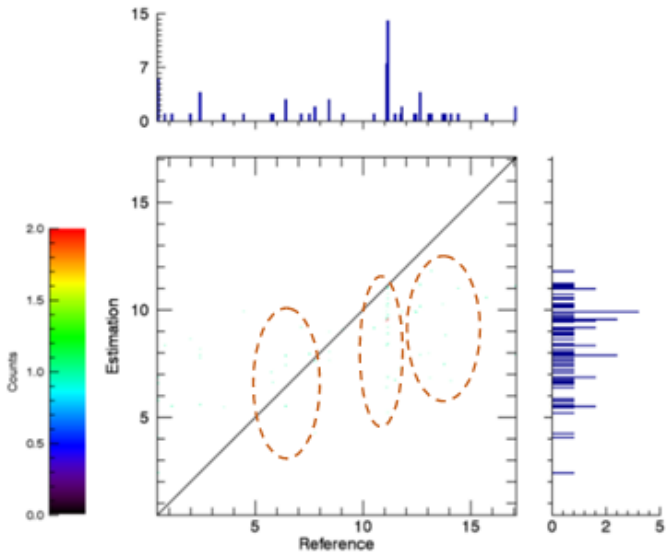

Figure 17. Graph of the validation reference against the RFR AGC estimation.

Band 5 was most frequently used in RF iterations, as depicted in the graph below (Figure 18). The specifications of the Band 5 Red (B5) with wavelength: 630 to 690 nm include: 1). Better focused on the absorption of red light by chlorophyll in healthy plant materials, 2). One of the most important bands for vegetation discrimination, 3). Very useful in classifying bare soils, roads, and geological features (DigitalGlobe 2009).

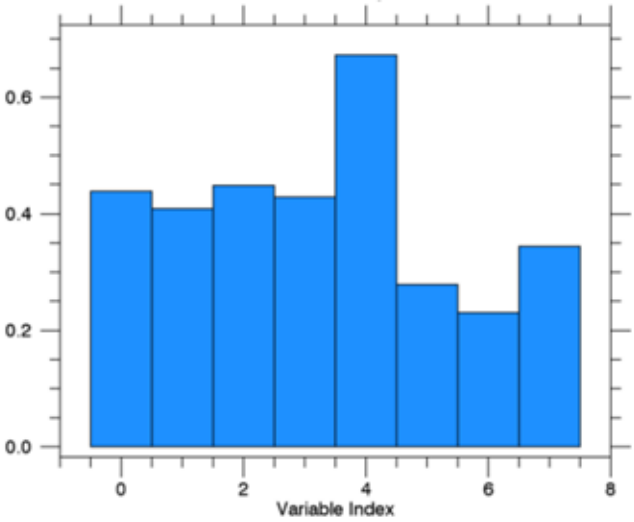

Figure 18. Normalized variable importance in the seagrass AGC model (the variable index stands for the color band, B1 to B8).

The RMSE analysis results, depicted above, suggested that modeling the AGC with a linear regression approach yielded a better outcome, although not statistically different, than modeling the AGC with an RFR model approach.

Discussion. This study used PCv as a rapid and non-destructive method to estimate the AGC of seagrass communities. Following the evaluation of the Manado City waters using the land cover categories, as outlined by Rahmawati et al (2017), the field survey recorded a medium-level seagrass coverage of 50.40% at the community level. Station 4 had the highest cover at 76.488%, with *T. hempricii* being the dominant species at 20.14%. In contrast, Station 1 had the lowest species coverage at 30.938%, with *H. ovalis* accounting for merely 0.21%, as the dominant species. A study by Togolo et al (2023) conducted around the ST5 (Tongkaina Village) area identified *T. hemprichii* as the type with the highest coverage percentage, reaching 30.08%.

The percentage of seagrass cover was obtained by B5 with R^2=0.32. PCv linear regression analysis of the seagrass map resulted in RMSE=25.61%, Pearson correlation *r*=0.59, and Squared Pearson correlation R^2=0.35. The linear regression mapping results showed the dominant seagrass PCv in the dense class (50-75%) located along the coastal waters. RFR Estimation Map resulted in RMSE=25.87%, Pearson correlation *r*=0.63, and Squared Pearson correlation R^2=0.40. The RF result indicated the dominant seagrass PCv in the dense class (50-75%) near the shoreline. This shows a different class than for the linear regression. Based on the RMSE values, the linear regression analysis results were better than those of RF.

Seagrass AGC was obtained with B2, by a linear regression analysis mapping at the community level, with R^2=0.37 with RMSE=3.70 g C m^{-2}, Pearson correlation *r*=0.57, and Squared Pearson correlation R^2=0.33. The results of linear regression mapping showed dominant seagrass AGC in the >9 g C m^{-2} class and were scattered along the coastal waters. RFR Estimation Map of AGC Seagrass resulted in RMSE=3.74 g C m^{-2}, Pearson correlation r=0.60, and Squared Pearson correlation R^2=0.36. The results of RF mapping had dominant seagrass AGC in the >9 g C m^{-2} class and were scattered along the coastal waters of Manado City, showing a different map class from the linear regression distribution's class. The linear regression analysis results outperformed the RF, as demonstrated by the RMSE values. Effectively using maps aids in communicating study results to stakeholders and the general public, thereby contributing to the conservation and management of seagrass ecosystems in the waters of Manado City. These efforts play a crucial role in bolstering the sustainability of marine environments and supporting initiatives aimed at mitigating climate change impacts. The accuracy of AGC seagrass mapping depends on three key factors, namely water brightness, the glint effect, and the timing of image acquisition during the lowest tides. These factors pose

challenges, particularly when image capture does not agree with field data collection. Future studies using multispectral imagery, such as the high-resolution WorldView-3 with 1.24 m multispectral capability, superior to WV2, offer promising solutions. This advanced technology enables sharper image acquisition, reducing errors caused by mud sediments covering seagrasses. Consequently, it minimizes the impact on reflectance values, crucial for the empirical model of seagrass AGC. This study focused solely on the assessment of AGC within the seagrass community, yielding a linear AGC mapping with RMSE=3.708 g C m^{-2}. In comparison, Wicaksono et al (2021) achieved a value of 5.41 g C m^{-2} with 58.79% accuracy, extending the investigation to the species level. To enhance accuracy, it is advisable to conduct further AGC mapping studies at the species level, as recommended by Wicaksono et al (2021). The regression equation developed in this study will significantly enhance the availability of seagrass AGC data, particularly for the species considered.

Conclusions. The current study estimated the seagrass carbon stocks in Manado City waters through remote sensing, by using the WV-2 high-resolution satellite imagery. The estimated value was 10.773 ton of AGC organic carbon with the average percentage of seagrass cover in the field being 50.40%, falling in the medium category with an area of ±133.11 ha. B5 has a PCv of seagrass with R^2=0.328, while the linear regression resulted in an RMSE=25.61%, Pearson correlation r=0.59 and Squared Pearson correlation R^2=0.35. Based on the results of linear regression mapping, the seagrass PCv predominated in the dense class (50–75%) and was found near coastal waters. RFR estimation map of seagrass PCv resulted in RMSE=25.873, Pearson correlation *r*=0.63, and Squared Pearson correlation R^2=0.40. The seagrass PCv observed in the RF results was predominantly found in the dense class (50–75%) near the shoreline. This RFR map was in a different class than with the linear regression. AGC seagrass obtained through B2 with R^2= 0.3759 and the linear regression analysis of mapping at the community level resulted in RMSE=3.70 g C m^{-2}, Pearson correlation r=0.57, and Squared Pearson correlation R^2=0.33. According to linear regression mapping results, seagrass AGC was distributed throughout coastal waters and was predominant in the >9 g C m^{-2} class. The map of RFR estimation of the seagrass AGC yielded RMSE=3.742 g C m^{-2} Pearson correlation r=0.60, and Squared Pearson correlation R^2=0.36. The RF mapping results showed that seagrass AGC was prominent in the >9 g C m^{-2} class, and was distributed across the coastal waters. The difference map between the plot of the results and the distribution was predicted by linear regression. The RMSE results on PCv and AGC showed that the linear regression analysis performed better than the RF. Based on the RF Variable Importance in the PCv and AGC image, B5 red was the band the most often used in iterations. The linear regression was identified as a better method than RF for seagrass AGC analysis, although the difference was not statistically significant.

Acknowledgements. The authors are grateful to all who contributed to enriching the results of this study, including the Manado City Government for granting access to satellite imagery through the Remote Sensing and Technology Center of the National Research and Innovation Agency (BRIN), as well as for their invaluable recommendations and educational funding support. The authors are also grateful to the Head of the Regional Forestry Service of North Sulawesi Province and the Head of Bunaken National Park (BTNB) for facilitating the access to the conservation area, as well as to the field survey team comprising Fichri Bacmid, Sarifudin Tidore, Syarifuddin, and Frengki Palendeng for the dedicated participation.

Conflict of interests. The authors declare no conflict of interest.

References

Acosta C., 1999 Benthic dispersal of Caribbean spiny lobsters among insular habitats: Implications for the conservation of exploited marine species. Conservation Biology 13(3):603-612.

Ampou E. E., Ouillon S., Iovan C., Andréfouët S., 2018 Change detection of Bunaken Island coral reefs using 15 years of very high resolution satellite images: A kaleidoscope of habitat trajectories. Marine Pollution Bulletin 131:83-95.
Baeza-Serrato R., Vázquez-López J. A., 2014 Transición de un modelo de regresión lineal múltiple predictivo, a un modelo de regresión no lineal simple explicativo con mejor nivel de predicción: Un enfoque de dinámica de sistemas. Revista Facultad de Ingenieria 71:59-71.
Bologna P. A. X., Heck K. L., 2002 Impact of habitat edges on density and secondary production of seagrass-associated fauna. Estuaries 25(5):1033-1044.
Bortone S. A., 2000 Seagrasses: monitoring, ecology, physiology, and management. CRC PRESS Boca 336:9-32.
Breiman L., 2001 Random forests. Machine Learning 45:5-32.
Green E. P., Mumby P. J., Edwards A. J., Clark C. D., 2000 Remote sensing handbook for tropical coastal management. In: Coastal management sourcebooks 3. Edwards A. J. (ed), Unesco Publishing 311:109-120.
Hedley J. D., Harborne A. R., Mumby P. J., 2005 Simple and robust removal of sun glint for mapping shallow-water benthos. International Journal of Remote Sensing. 25(10):2107-2112.
Hogarth P., 2007 The biology of mangroves and seagrasses. Oxford University Press 289:44-52.
Humphries P., 1991 Utilization of the shallows of a south-western Australian estuary by fish, with special reference to the influence of the aquatic macrophyte *Ruppia megacarpa*. Dissertation, Murdoch University, Australia, 125 p.
Hossain M. S., Bujang J. S., Zakaria M. H., Hashim M., 2015 The application of remote sensing to seagrass ecosystems: an overview and future research prospects. International Journal of Remote Sensing 36(1):61-114.
Ilyas T. P., Nababan B., Madduppa H., Kushardono D., 2020 Seagrass ecosystem mapping with and without water column correction in Pajenekang Island waters, South Sulawesi. Jurnal Ilmu dan Teknologi Kelautan Tropis 12:9-23.
Kendrick A. J., 2002 Resource utilisation and reproductive biology of syngnathid fishes in a seagrass-dominated marine environment in south-western Australia. Dissertation, Murdoch University, Australia, 156 p.
Kay S., Hedley J. D., Lavender S., 2009 Sun glint correction of high and low spatial resolution. Remote Sensing 1(4):697-730.
McKenzie L. J., Campbell S. J., Roder C. A., 2003 Seagrass-watch: Manual for mapping and monitoring seagrass resources. 2nd Edition. CRV Reef, Townsville, 100 p.
McKenzie L. J., 2003 Guidelines for the rapid assessment and mapping of tropical seagrass habitats. Seagrass-Watch HQ, http://www.seagrasswatch.org/Methods/Manuals/SeagrassWatch_Rapid_Assessment_Manual.pdf
Mckenzie L., Yoshida R., 2009 Seagrass-Watch: proceedings of a workshop for monitoring seagrass habitats in Indonesia. The Nature Conservancy, Coral Triangle Center, Sanur, Bali, Seagrass-Watch HQ, 56 p.
Merryanto Y., Kase A. G. O., 2022 The diversity of fish in seagrass beds and bare sand channel in Tablolong Waters, Kupang Regency. Ecology, Environment & Conservation 28:S121-S125.
Misbari S., 2017 Quantification of submerged seagrass total aboveground biomass for Malaysian coastal waters using remote sensing data. Environment Science, https://api.semanticscholar.org/CorpusID:134167323
Nadiarti N., Riani E., Djuwita I., Budiharsono S., Purbayanto A., Asmus H., 2012 Challenging for seagrass management in Indonesia. Journal of Coastal Develpopment 15(3):1410-5217.
Nienhuis P. H., 2002 Global seagrass research methods. Elsevier, Amsterdam. Aquaculture 212:405-407.
Pal M., 1996 Random forests for land cover classification mahesh pal department of civil engineering National Institute of Technology, Kurukshetra. Symposium a Quarterly Journal In Modern Foreign Literatures, pp. 3510-3512.
Rahman W., Wicaksono P., 2019 Application of WorldView-2 imagery for bathymetry

mapping in Kemujan Island, Karimunjawa National Park. Jurnal Penginderaan Jauh Indonesia 1(1):333-338.
Rahmawati S., Irawan A., Supriyadi I. H., Azkab M. H., 2017 Seagrass meadow condition assessment monitoring guide. COREMAP-CTI Indonesian Institute of Sciences, 35 p.
Rais M., Inaku D. F., Moka W. J. C., Mashoreng S., Satari D. Y., Rukminasari N., 2023 Seagrass carbon stock estimation using spot-7 imagery in the waters of Kodingarenglompo Island, Sangkarrang, Makassar City. Jurnal Kelautan Tropis 26(2):387-398.
Roelfsema C. M., Lyons M., Kovacs E. M., Maxwell P., Saunders M. I., Samper-Villarreal J., Phinn S. R., 2014 Multi-temporal mapping of seagrass cover, species and biomass: A semi-automated object based image analysis approach. Remote Sensing of Environment 150:172-187.
Savini A., Vrazi A. G., Marino L., Fersini G., Piazzolla D., Scanu S., Marcelli M., 2023 Geospatial modeling for evaluating restoration suitability of Posidonia oceanica meadows offshore Civitavecchia (eastern Tyrrhenian margin, Mediterranean Sea). EGU General Asembly Vienna, Austria, EGU23-14936.
Sondak C. F. A., Kaligis E. Y., 2022 Assessing the seagrasses meadows status and condition: A case study of Wori seagrass meadows, North Sulawesi, Indonesia. Biodiversitas 23(4):2156-2166.
Supriyadi I. H., Alifatri L. O., Kusnadi A., Hafizt M., Lisdayanti E. 2023 Current status of seagrass condition in coastal waters of Kendari Southeast Sulawesi Indonesia. IOP Conference Series: Earth and Environmental Science 1137(1):012-015.
Tamondong A. M., Cruz C. A., Guihawan J., Garcia M., Quides R. R., Cruz J. A., Blanco A. C., 2018 Remote sensing-based estimation of seagrass percent cover and LAI for above ground carbon sequestration mapping. Proceedings Remote Sensing of the Open and Coastal Ocean and Inland Waters 10778.
Togolo F., Menajang F. S. I., Manginsela F. B., Kondoy K. I. F., Lasabuda R., Schaduw J. N., 2023 Status of seagrass beds in the Bahowo Waters, Manado City North Sulawesi Province. Jurnal Ilmiah Platax 11:6-14.
Uku J., Daudi L., Muthama C., M., Alati V., Kimathi A., Ndirangu S., 2021 Seagrass restoration trials in tropical seagrass meadows of Kenya. Western Indian Ocean Journal of Marine Science 2(2):69-79.
Wicaksono P., 2016 Improving the accuracy of multispectral-based benthic habitats mapping using image rotations: The application of principle component analysis and independent componentanalysis. European Journal of Remote Sensing 49:433-463.
Wicaksono P., Hafizt M., 2013 Mapping seagrass from space: Addressing the complexity of seagrass LAI mapping. European Journal of Remote Sensing 46(1):18-39.
Wicaksono P., Lazuardi W., Munir M., 2019a Integrating image at different spatial resolutions and field data for seagrass percent cover mapping. International Archives of the Photogrammetry, Remote Sensing and Spatial Information Sciences-ISPRS Archives 42:487-492.
Wicaksono P., Aryaguna P. A., Lazuardi W., 2019b Benthic habitat mapping model and cross validation using machine-learning classification algorithms. Remote Sensing 11(11):1279.
Wicaksono P., Danoedoro P., Hartono, Nehren U., Maishella A., Hafizt, M., Arjasakusuma S., Harahap S. D., 2021 Analysis of field seagrass percent cover and aboveground carbon stock data for non-destructive aboveground seagrass carbon stock mapping using worldview-2 image. International Archives of the Photogrammetry, Remote Sensing and Spatial Information Sciences-ISPRS Archives 46:321-327.
Wicaksono P., Harahap S. D., 2023 Mapping seagrass biodiversity indicators of Pari Island using multiple worldview-2 bands derivatives. Geosfera Indonesia 8(2):189-205.
Wagey B. T., Paruntu C., Lasabuda R., Kambey A., 2023 Short communication: Diversity, biomass, and carbon stock of seagrass community in three coastal waters of Minahasa Peninsula, North Sulawesi, Indonesia. Biodiversitas 24(3):1793-1798.
*** DigitalGlobe, 2009 The benefits of the 8 spectral bands of worldview-2, white paper. http://worldview2.digitalglobe.com/docs/WorldView-2_8-Band_Applications_Whitepaper.pdf

*** DigitalGlobe, 2016 Data sheet worldview-2. digitalglobe, DS-WV2 07/16, https://dg-cms-uploads-production.s3.amazonaws.com/uploads/document/file/98/WorldView2-DS-WV2-rev2.pdf
*** ENVI, 2009 ENVI atmospheric correction module: QUAC and FLAASH user's guide. Module Version.
*** Government of Indonesia, 2014 Regulation of the Minister of Environment and Forestry of the Republic of Indonesia No. SK. 734/Menhut-II/2014 on Forest and Aquatic Conservation Areas of North Sulawesi Province. Jakarta, Indonesia.
*** HGIA, Head of Geospatial Information Agency, 2018 Regulation No. 6/2018 on the Amendment to the Head of Geospatial Information Agency Regulation No. 15/2014 on Technical Guidelines for Base Map Accuracy, Badan Informasi Geospasial. Bogor, Indonesia.
*** Manado Municipal Government, 2023 Regional Regulation Number 1 of 2023 concerning the Regional Spatial Plan of Manado City (RTRW) for the years 2023-2042. Manado, Indonesia.
*** North Sulawesi Province, 2017 Regional Regulation of North Sulawesi Province Number 1 of 2017 concerning the Zoning Plan for Coastal Areas and Small Islands of North Sulawesi Province (RZWP3K). Manado, Indonesia.
*** UNEP/GEF, 2004 Regional working group on seagrass of the UNEP/GEF Project entitled Reversing environmental degradation trends in the south china sea and gulf of Thailand. UNEP/GEF/SCS Technical Publication. Seagrass in the South China Sea 3:16.

Received: 05 February 2024. Accepted: 02 April 2024. Published online: 17 April 2024.
Authors:
Maxi Willem Solang, Marine Science Doctoral Study Program, Faculty of Fisheries and Marine Sciences Sam Ratulangi University, Manado 95115, North Sulawesi, Indonesia, e-mail: willemsolang@gmail.com
Rene Charles Kepel, Faculty of Fisheries and Marine Science, Sam Ratulangi University, Manado 95115, North Sulawesi, Indonesia, e-mail: renecharleskepel65@gmail.com
Kakaskasen A. Roeroe Faculty of Fisheries and Marine Science, Sam Ratulangi University, Manado 95115, North Sulawesi, Indonesia, e-mail: andreasroeroe@unsrat.ac.id
Pramaditya Wicaksono, Cartography and Remote Sensing, Faculty of Geography Universitas Gadjah Mada, Sekip Utara, Yogyakarta 55281, Indonesia, e-mail: prama.wicaksono@geo.ugm.ac.id
Winda Mercedes Mingkid, Sam Ratulangi University, Faculty of Fisheries and Marine Science Unsrat, Kampus Unsrat Bahu St., Manado 95115, North Sulawesi, Indonesia, e-mail: wmingkid@unsrat.ac.id
Franky Erens Kaparang, Ratulangi University, Faculty of Fisheries and Marine Science Unsrat, Kampus Unsrat Bahu St., Manado 95115, North Sulawesi, Indonesia, e-mail: frangky_kaparang@yahoo.com
Desy Maria Helena Mantiri, Marine Science Study Program, Graduate School of, Sam Ratulangi University, 95115 Manado, Indonesia, e-mail: dmh_mantiri@unsrat.ac.id
Kurniati Kemer, Marine Science Study Program, Faculty of Fisheries and Marine Science, Sam Ratulangi University, 95115 Manado, Indonesia, e-mail: kurnikemer@unsrat.ac.id
Muhammad Hafizt, Research Center for Oceanography-Research and Innovation Agency, Indonesia (RCO-BRIN), e-mail: muhammadhafizt@gmail.com
Huwaida Nur Salsabila, Cartography and Remote Sensing, Faculty of Geography Universitas Gadjah Mada, Sekip Utara, 55281 Yogyakarta, Indonesia e-mail: huwaidans@gmail.com

How to cite this article:
Solang M. W., Kepel R. C., Roeroe K. A., Wicaksono P., Mingkid W. M., Kaparang F. E., Mantiri D. M. H., Kemer K., Hafizt M., Salsabila H. N., 2024 Assessment of seagrass percent cover and aboveground carbon stock using linear and random forest regression based on Worldview-2 satellite imagery in Manado City waters, North Sulawesi Province, Indonesia. AACL Bioflux 17(2):723-743.